Statistics of Seismicity to Investigate the Campi Flegrei Caldera Unrest

Anna Tramelli (anna.tramelli@ingv.it)
National Institute of Geophysics and Volcanology
Cataldo Godano
University of Campania "Luigi Vanvitelli"
Patrizia Ricciolino
National Institute of Geophysics and Volcanology
Flora Giudicepietro
National Institute of Geophysics and Volcanology
Stefano Caliro
National Institute of Geophysics and Volcanology
Massimo Orazi
National Institute of Geophysics and Volcanology
Prospero De Martino
National Institute of Geophysics and Volcanology
Giovanni Chiodini
National Institute of Geophysics and Volcanology

Research Article

Keywords: Campi Flegrei calderic system, volcanic risk, seismicity rate, gas composition

Posted Date: January 27th, 2021

DOI: https://doi.org/10.21203/rs.3.rs-152574/v1

Version of Record: A version of this preprint was published at Scientific Reports on March 30th, 2021. See the published version at https://doi.org/10.1038/s41598-021-86506-6.

Statistics of seismicity to investigate the Campi Flegrei caldera unrest

A. Tramelli [a], C. Godano [b,a], P. Ricciolino[a], F. Giudicepietro[a], S. Caliro [a], M. Orazi [a], P. De Martino [a] and G. Chiodini[a]

[a]Istituto Nazionale di Geofisica e Vulcanologia, Osservatorio Vesuviano, Napoli, Italy

[b]Department of Mathematics and Physics, University of Campania "Luigi Vanvitelli", Caserta, Italy

[*]Corresponding author: Anna Tramelli, anna.tramelli@ingv.it

January 22, 2021

Abstract

The knowledge of the dynamic of the Campi Flegrei calderic system is a primary goal to mitigate the volcanic risk in one of the most densely populated volcanic areas in the world. From 50s to 80s Campi Flegrei suffered three bradyseismic crises with a total uplift of almost 4.3 m. After a period of subsidence of 20 years, the uplift started again in 2005 accompanied by a low increment in the seismicity rate. In 2012 an increment in the seismic energy release and a variation in the gas composition of the fumaroles of Solfatara (in the central area of the

caldera) were recorded. Since then, a slow and progressive increase in phenomena continued until today. We analyze the seismic catalogue of Campi Flegrei from 2000 to 2020 collected by INGV - Osservatorio Vesuviano to look for any variation in the seismic parameters and compare them with geochemical monitored ones. A remarkable correlation between independent variables as earthquake cumulative number, CO/CO_2 values and vertical ground deformation reveals a likely common origin. The interpretation of the seismological, geochemical and geodetical observable brings back to the injection of magmatic fluids into the hydrothermal system or its pressurization.

1 Introduction

Within the bradyseismic phenomenon which characterize the Campi Flegrei volcanic field (figure 1), an uplift of the central part of the caldera has been recorded since 2005, reaching a value of 65 cm at the beginning of 2020. Referring to what the history of this volcano can teach us, the last eruption of Campi Flegrei occurred in 1538 on the western side of a raised marine terrace, and from historical and geological reconstructions, the seismicity and uplift had been increasing for about one hundred years before the eruption. Some days before the eruption a rapid and localized increase in the uplift occurred (Guidoboni and Ciuccarelli, 2011; Acocella et al., 2015). A slow subsidence occurred possibly for most of the period since the eruption. Uplift episodes are documented in 1950-52, 1969-72 and 1982-84 (Del Gaudio et al., 2010). The last one was associated to a total uplift of 1.8 m in the central area of the caldera with the occurrence of more than 16000

earthquakes (Orsi et al., 2004) without culminating in an eruption.

After a subsidence of more than 20 years, the caldera uplift started again in 2005 (De Martino et al., 2014) together with an increment in the seismicity rate (D'Auria et al., 2011) and in the degassing activity (Chiodini et al., 2015). An increment in the seismic energy released occurred in 2012 (see figure 2). After a brief period of quiet, uplift resumed in 2014, the seismicity become shallower (<2km) and its rate increased again (Chiodini et al., 2017; Giudicepietro et al., 2019).

Uplift, seismicity and gas-composition of the hydrothermal system are showing variations that needs to be faced to understand a possible evolution of the volcanic system. We statistically analyze the seismic catalogue of Campi Flegrei from 2000 to 2020 to understand the temporal variations of inter-time and inter-space between earthquakes and to correlate them with the trend of the geochemical parameters and deformations.

2 Method

We analyzed the seismic catalogue of Campi Flegrei constantly updated from INGV - Osservatorio Vesuviano. We considered the time window from August 2000 to April 2020. The catalogue contains earthquake time, location, M_d and location errors.

The magnitude of the Campi Flegrei seismic catalogue is evaluated by the coda duration measured at a short-period seismic station located at the Solfatara crater (STH). The duration-magnitude empirical relation can be found in Orsi et al. (2004). The same relationship and station have been

used since 1984 ensuring a stable and stationary method for magnitude estimation.

Each event is detected and located automatically or, eventually, by the shift workers present in the monitoring room of Osservatorio Vesuviano 24H/day. Successively, each earthquake is manually revised by the seismic laboratory and inserted into the official catalogue here considered.

2.1 The theoretical sensibility of the seismic network with time

The detection threshold of any seismic network can be characterized by the completeness magnitude M_c. For magnitudes larger than M_c the network is able to detect any earthquake occurring in the area, conversely, not all the events with magnitude smaller than M_c are detected. As a consequence, the number of earthquakes with a magnitude smaller than M_c reported in the catalogues is smaller than what expected by the Gutenberg-Richter relationship.

Analyzing a seismic catalogue M_c is usually estimated with different techniques: the maximum curvature method (Wiemer and Wyss, 2000), Goodness-of-Fit Test (Wiemer and Wyss, 2000), b-value stability approach (Cao and Gao, 2002), Entire Magnitude Range (Ogata and Katsura, 1993; Woessner and Wiemer, 2005), and others. To take into account the improvement of the Campi Flegrei seismic network with time we used a theoretical method that allows to define the detection and location sensibility in space of a seismic network (Tramelli et al., 2013; Orazi et al., 2013) and apply it for different time windows. The method consists in simulating earthquakes

with different magnitudes distributed on a grid at a certain depth. More precisely, a grid of synthetic earthquakes, located in the area plotted in figure 3 at a depth of 1 km b.s.l., has been generated with the following source and medium parameters: stress drop of 0.5 MPa (using the Brune (1970) source model), average rock density of 2000 kg/m^3 (Del Pezzo et al., 1987)) mean quality factor Q=100 (Petrosino et al., 2008). The seismic noise at each station has been evaluated as the mean daily noise. The magnitude threshold for location is defined as the minimum magnitude of an earthquake recordable by at least 4 seismic stations. The same method is used for the detection threshold but the number of stations recording the earthquakes has to be larger than 1.

As we are considering the seismic catalogue of the located earthquakes we assume that the location sensitivity of the network in the epicentral area represents a theoretical evaluation of Mc. For the analysis we considered the time periods indicated in figure 3 and the seismic stations operating for most of the referring period.

Figure 3 shows that the number of seismic stations increased with time (blue triangles) and the network performances has been improved in parallel enlarging the location area. To allow a better understanding of the proposed image we also plot the earthquakes with magnitude smaller than 0.2 recorded in the referring period. This analysis allows us to define a M_c range between 0 and 0.5 in the inner part of the caldera for the whole analysed period.

2.2 The temporal variations of b and the empirical evaluation of M_c

As a first step we estimate the temporal variations of the Gutenberg-Richert b parameter. The analysis has been performed dividing the catalogue in moving time windows with different lengths, going from 100 to 350 earthquakes to analyse the influence of this window on the b value estimation as suggested by Greenfield et al. (2020). As can be seen in figure 4 the b value tends to assume smaller values for larger window size and shows higher variations for smaller window sizes. Our main interest is in these variations to be compared to the trend of other variables. As a consequence we decide to use a window of 150 events representing a good compromise. Moreover the simulation, described in the Supplementary Materials, reveals that using 150 events it is possible to obtain a reliable estimation of the b value. Due to the small occurrence rate of earthquake in the first part of the analyzed catalogue, taking a window length of 100 earthquakes the first sample point with magnitude above 0.2 occurs in 2010. With a window length of 350 earthquakes the first sample occurs in 2016. In order to perform our analisys for the longest as possible time period, we decided to start with windows of 75 earthquakes with one earthquake shift and increasing the number till 150 in the successive windows. We show the complete time series including the 75-to-150 samples part. Even if the first part of the results is affected by higher errors, this procedure allows us to show the trends from 2010. Anyway, we will focus the analysis to the time series starting from 2014.

For each time window we estimate the M_c and the b value minimizing the

residuals of the Gutenberg-Richter fit (Cao and Gao, 2002), and we analyse the residuals associated to the b value with respect to the M_c variations. The obtained M_c values span from -0.2 to 0.4, with some points at 0.8. However the M_c variation does not exhibit any trend enlightening that there is no evidence of a visible improvement of the M_c estimates in the epicentral area since 2012. From the sensibility analysis we notice that after 2011 the sensibility location threshold of the central part of the caldera remain almost constant, confirming the empirical data. Moreover we observe that, if we use two different values of the completeness magnitude, namely M_c=0.2 and M_c=0.4, the b parameter variation trend does not exhibit any substantial difference. Even if the b value assumes smaller values for M_c=0.2 in respect of M_c=0.4, the trend and the variation points are the same (figure 4). Finally, we decided to fix M_c=0.2 for any analyzed window. The reasons for this choice are deeply discussed in the Supplementary Materials.

To evidence possible different behaviour of the seismogenic structures, in addition to the b value, we evaluate the average intertime between successive earthquakes Δt, the average epicentral interdistance ξ between all the possible couple of the 150 earthquakes weighted for the location horizontal error and the average depth ζ weighted for the vertical location error.

The b values are estimated using the maximum likelihood method (Aki, 1965) and their errors are estimated using the Shi and Bolt (1982) formula. The error in the b value estimation due to the use of the M_d has been extensively described in the Supplementary Material and is almost equivalent to the one estimated using Shi and Bolt (1982).

The obtained seismological time series are finally compared with inde-

pendent compositional data of the main fumarolic emission of Campi Flegrei (i.e. "Bocca Grande" fumarole, BG in figure 1) that showed important variations interpreted as due to heating and pressurization of the feeding hydrothermal system (Chiodini et al., 2015, 2017; Giudicepietro et al., 2019). Among the many monitored parameters, we will refer in particular to the CO/CO_2 fumarolic ratio that is the best indicator of the ongoing heating process (Chiodini et al. (2015) and references there in).

3 Results

The analysis of the M_c shows that its value remains almost constant in the last 10 years. Despite the network has been improved, the new stations were deployed mainly in the western border of the caldera and in its sea side enlarging the area covered by the network and allowing to evidence a possible ipocentral migration and to improve the location error. Otherwise the area where the seismicity mainly occurs is close to the Solfatara crater (figure 1) that has been well covered by the network since 2010. Except for some isolated earthquakes, the seismicity is indeed occurring in the central part of the caldera close to the Solfatara crater; differently from what recorded during the 1982-84 bradyseismic crises when earthquakes were scattered within the whole caldera.

In 2005 a new uplift started in Campi Flegrei caldera together with an increment in the seismicity and a variation in the gas composition emitted at the Solfatara fumarolic vents. The uplift has a bell shape centered in the town of Pozzuoli (Rione Terra) where the elevation reached 65 cm at the

beginning of 2020. The uplift started slowly, 1-2 cm per year, till 2012 when it moved up to 6-7 cm per year. The temporal evolution of these phenomena, together with the variations in the gas composition of the monitored fumaroles, leaded the Civil Defence of Italy to move the alert state of the volcano from green to yellow in 2012.

In volcanic areas the seismicity is related to the presence of fluids, to the rheology of the crust, and to the local stress fields (D'Auria et al., 2015). Its increasing rate and energy released, together with surface deformation, and degassing, is used to define caldera unrests (Acocella et al., 2015; Giudicepietro et al., 2017). Seismicity is usually described using occurrence rate, magnitude and the Gutenberg-Richter b value. In volcanic areas the magnitude is usually low to moderate and the b value is higher than 1, due to the presence of fluids within a highly fractured rock. Concerning the Campi Flegrei area, Siniscalchi et al. (2019) estimated the b value for the period 2005-2016 founding a value of 0.92 and a value of 1.03 is found by Giudicepietro et al. (2019) for the period 2005-2019. Comparing them with the value of 0.72 found for the period 1983-1984 by D'Auria et al. (2011), such a low value can be related to high stress regimes (Farrell et al., 2009). It is interesting to notice that, during the 1982-84 bradiseismic crises the seismicity was spread over the caldera inner and the b value was very low ($\simeq$0.5-0.6) for earthquakes located in the South-West part of the caldera and slightly higher ($\simeq$0.7) for earthquakes located closer to the Solfatara area (D'Auria et al., 2011). From August 2000 to April 2020 about 1700 earthquakes have been recorded. Most of them are located in the Solfatara/Pisciarelli area and we estimated a b value of 0.92 ± 0.03 for the whole period. The seismicity

is moderate but, taking into account the 20 years of the analyzed catalogue, from December 2019 to April 2020 more than the 70% of the total energy have been released (line blue in figure 2).

The b value increases from values smaller than 0.8 in 2012 to values close to 1.3 at the end of 2019 (figure 5a). Periods of variability are identifiable at the beginning of 2018 and at the end of 2019 when it again increases reaching values close to 1.3 (figure 5a). This increment could be associated to high pore pressure possibly induced by magmatic fluids injection (Farrell et al., 2009). When magmatic fluids intrude, the temperature around them rises weakening the crust which is unable to accumulate high stress. Weakened crusts as well as expanding sills (Giudicepietro et al., 2016; Macedonio et al., 2014) could generate numerous small fractures and, consequently, the b value increment.

The evolution of the average intertime between earthquakes (figure 5b) evidences that the seismicity is getting closer with time. At the beginning of the analyzed catalogue the average intertimes assumed values of several hours with huge standard deviations. As well as the time goes on, both average values and standard deviations decrease. This reveals that the clustering regime persists with time. Indeed, the clustering degree can be characterized by the c_V defined as $c_V = \frac{\sigma}{\langle \Delta t \rangle}$ being σ the standard deviation and $\langle \Delta t \rangle$ the average value. c_V assumes a value equal to 0 for periodic occurrence, equal to 1 for Poissonian occurrence and > 1 for clustered events. For the analyzed catalogue c_V ranges from 1.8 to 2.2. A stationary $c_V > 1$ implies a constant clustering degree even if a decreasing $\langle \Delta t \rangle$ (its value decreases with time till values of several dozens of seconds in 2019) indicates the oc-

currence of denser swarms separated in time. The inter-space trend, shown in figure 5c, enlightens the increment of the earthquake spatial clustering with time. Being the earthquakes in a swarm always close to each others, it shows that the swarms become closer in space. The inter-space goes from values of 2.2 km to 1.2 km with a mean error of the epicentral location of a few hundred meters. The average depth (figure 5d) decreases with time; the evident steps in the trend are related to the occurrence of new swarms. The δ value moves from 2 km to 1.2 km.

All the dynamics is signed by the occurrence of earthquake swarms. A first step is identifiable in September 2012 when a seismic swarm with $M_{max} = 1.7$ occurred. We are not going to discuss it because it is at the very beginning of our temporal series and is followed by a seismic quiescent period. However, we underline that it is the only swarm in the analyzed period located close to the area of the maximum elevation (Pozzuoli harbor) at almost 2 km from the Solfatara/Pisciarelli area. The second step in the intertime is identifiable in 2015 coinciding with the swarm of the October 7, 2015. At the same time we notice a decrease in the average interdistance and in the average depth. This swarm occurred at the end of a period of uplift increment that stopped in coincidence with the swarm itself. The successive step occurred in July 2016 in coincidence with another swarm (54 detected earthquakes, $M_{max} = 2.1$) Giudicepietro et al. (2020). Again it occurred after an increment in the caldera uplift exhibiting the same trend of the curves (decrement of the interdistance and mean depth and an increment in the CO/CO_2, figure 6), as observed for the previous swarm. For both the swarms the b value remains almost constant. At the end of 2017 two little

swarms ($M_{max} = 0.9$) were recorded in the area of Solfatara/Pisciarelli and an increment in the b value is detectable. At the same time the interdistance and the mean depth are decreasing. The CO/CO_2 showed a marked change in its trend (figure 6) and also the uplift started again to increase after a stable period. From the end of 2018 to middle 2019 the b value showed a slightly decrement while mean depth and interdistance exhibit tiny variations in the trend. Another noticeable step occurs at the end of 2019 with the swarm of December 6, 2019. Here the earthquakes become shallower but, differently from the previous behavior, they slightly spread away. Anyway, except for the 2012 swarm, all the swarms are located close to the area of Solfatara/Pisciarelli.

In order to enlighten common features in the analyzed variables we present all the variables on the same plot (figure 7) where we show also the vertical uplift of the central part of the caldera, the CO/CO_2 ratio and the cumulative number of events. It is evident that all the curves exhibit very similar behaviours. Indeed, plotting each variable versus the others, we observe a clear dependence of each variables on the others. Figure 8 shows three examples of these dependence (the others are shown in the Supplementary Materials). We would like to remark here that the functional form of the dependence of each variable on the other is less relevant in this study than the existence of the dependence itself. This, in fact, reveals that all the temporal variation of our observable can be leaded back to a common cause, namely the fluid heating or pressurization clearly revealed by the CO/CO_2 increase in time. This quantity is remarkably correlated with the cumulative number of events and the ground vertical deformation (see figures 6 and 8)

enlightening a common cause for the temporal variations of the investigated variables.

Taking into account all the variations we suggest that the common cause can be identifiable with fluid injection or pressurization. Injection of magmatic fluids within the hydrothermal system which feeds the Solfatara/Pisciarelli fumaroles would heat up the system increasing the pore pressure and facilitating the earthquakes occurrence being the medium less prone to bear stress and being the faults lubricated. Considering the vertical uplift the surficial manifestation of a deeper crustal bending, it could plays both as cause and consequence in this process being induced by the heating of the hydrothermal system and inducing fracture generation which recalls fluids towards the surface. A slightly decrement in the V_s velocity, compatible both with fluid presence and temperature increment, was evidenced by Zaccarelli and Bianco (2017) using the cross correlation of the seismic noise recorded in the caldera.

4 Conclusions

The seismological and geochemical anomalies recorded in Campi Flegrei can be interpreted in terms of magmatic fluid circulation and permeability increment within the hydrothermal system. A magmatic intrusion or the injection of magmatic fluids were claimed as cause of the variations recorded from the beginning of the uplift until the 2012 (D'Auria et al., 2015; Chiodini et al., 2017), but starting from middle 2018 the behaviour of the system showed a clear variation. The available tomographies (e.g. Calò and Tramelli, 2018;

Zollo et al., 2003) evidence that a seismic layer, characterized by low V_p/V_s and low attenuation, was located at a depth of ~ 2.5 km, where most of the seismicity occurred. Its rheological properties could have possibly suffered little variations due to vertical movement and heating. Geochemical analysis show that the gases involved in the hydrothermal system and sampled at the Solfatara/Pisciarelli fumarolic vents originate from a higher pressured system.

The rheological conditions of the central part of the caldera seems to be changing in time. Different rheological behaviours at Campi Flegrei have already been observed several times during the unrest and volcanic episodes occurred over the last 15 kyr (Vitale et al., 2019). Successions of brittle structures such as faults in contrast with levels of water saturated loose sands have been observed within the Campi Flegrei caldera. An increment in the temperature could recall hot fluids from the lower system increasing the pore pressures and lubricating the faults facilitating earthquake occurrence. The increment of the b value observed in the last decade as well as more dense and superficial swarms are compatible with the this hypothesis. These observables temporal change appears to be correlated among themselves and with the ground deformations evidencing a variation in the hydrothermal system supported also by the increment in the CO/CO_2 fumarolic ratio. In particular, the last quantity signs an increase of the temperature of the hydrothermal system since the end of 2017 that could be interpreted as due to fluid injection into the system or their pressurization. The CO/CO_2 fumarolic ratio is remarkably correlated with the earthquakes cumulative number since 2000 (figure 6) indicating that a further increment could affect

both the volcanological and seismological hazard.

Acknowledgements

The authors acknowledge financial support of the PRIN-2017 Stochastic forecasting in complex systems. The author wish to thank all the many colleagues who contribute daily to the monitoring of Campi Flegrei. This paper does not necessarily represent the Italian Department of Civil Defence (DPC) official opinion and policies.

5 Data Availability

The seismic catalog is available at the website of Osservatorio Vesuviano: http://sismolab.ov.ingv.it/sismo/. All the other data used in the article are available under request to the corresponding author.

References

Acocella, V., Di Lorenzo, R., Newhall, C., Scandone, R., 2015. An overview of recent (1988 to 2014) caldera unrest: Knowledge and perspectives. Reviews of Geophysics 53 (3), 896–955.

Aki, K., 1965. Maximum likelihood estimate of b in the formula log n= a-bm and its confidence limits. Bull. Earthq. Res. Inst., Tokyo Univ. 43, 237–239.

Brune, J. W., 1970. Tectonic stress and the spectra of the seismic shear waves from earthquakes. J. Geophys. Res. 75, 4997–5009.

Calò, M., Tramelli, A., 2018. Anatomy of the campi flegrei caldera using enhanced seismic tomography models. Scientific reports 8 (1), 1–12.

Cao, A., Gao, S. S., 2002. Temporal variation of seismic b-values beneath northeastern japan island arc. Geophysical research letters 29 (9), 48–1.

Chiodini, G., Selva, J., Del Pezzo, E., Marsan, D., De Siena, L., D Auria, L., Bianco, F., Caliro, S., De Martino, P., Ricciolino, P., et al., 2017. Clues on the origin of post-2000 earthquakes at campi flegrei caldera (italy). Scientific reports 7 (1), 4472.

Chiodini, G., Vandemeulebrouck, J., Caliro, S., D'Auria, L., De Martino, P., Mangiacapra, A., Petrillo, Z., 2015. Evidence of thermal-driven processes triggering the 2005–2014 unrest at campi flegrei caldera. Earth and Planetary Science Letters 414, 58–67.

D'Auria, L., Giudicepietro, F., Aquino, I., Borriello, G., Gaudio, C. D., Bascio, D. L., Martini, M., Ricciardi, G. P., Ricciolino, P., Ricco, C., 2011. Repeated fluid-transfer episodes as a mechanism for the recent dynamics of Campi Flegrei caldera (19892010). J. Geophys. Res. 116 (B04313), doi:10.1029/2010JB007837.

D'Auria, L., Massa, B., Cristiano, E., Del Gaudio, C., Giudicepietro, F., Ricciardi, G., Ricco, C., 2015. Retrieving the stress field within the campi flegrei caldera (southern italy) through an integrated geodetical and seismological approach. Pure and Applied Geophysics 172 (11), 3247–3263.

De Martino, P., Tammaro, U., Obrizzo, F., 2014. Ps time series at campi flegrei caldera (2000-2013). Annals of geophysics 57 (2), 0213.

Del Gaudio, C., Aquino, I., Ricciardi, G., Ricco, C., Scandone, R., 2010. Unrest episodes at campi flegrei: A reconstruction of vertical ground movements during 1905–2009. Journal of Volcanology and Geothermal Research 195 (1), 48–56.

Del Pezzo, E., De Natale, G., Martini, M., Zollo, A., 1987. Source parameters of microearthquakes at phlegraean fields (Southern Italy) volcanic area. Phys. Earth Planet. Interiors 47, 25–42.

Farrell, J., Husen, S., Smith, R. B., 2009. Earthquake swarm and b-value characterization of the yellowstone volcano-tectonic system. Journal of Volcanology and Geothermal Research 188 (1-3), 260–276.

Giudicepietro, F., Chiodini, G., Caliro, S., De Cesare, W., Esposito, A. M., Galluzzo, D., Lo Bascio, D., Macedonio, G., Orazi, M., Ricciolino, P.,

et al., 2019. Insight into campi flegrei caldera unrest through seismic tremor measurements at pisciarelli fumarolic field. Geochemistry, Geophysics, Geosystems 20 (11), 5544–5555.

Giudicepietro, F., López, C., Macedonio, G., Alparone, S., Bianco, F., Calvari, S., De Cesare, W., Delle Donne, D., Di Lieto, B., Esposito, A. M., et al., 2020. Geophysical precursors of the july-august 2019 paroxysmal eruptive phase and their implications for stromboli volcano (italy) monitoring. Scientific reports 10 (1), 1–16.

Giudicepietro, F., Macedonio, G., D'Auria, L., Martini, M., 2016. Insight into vent opening probability in volcanic calderas in the light of a sill intrusion model. Pure and Applied Geophysics 173 (5), 1703–1720.

Giudicepietro, F., Macedonio, G., Martini, M., 2017. A physical model of sill expansion to explain the dynamics of unrest at calderas with application to campi flegrei. Frontiers in Earth Science 5, 54.

Greenfield, T., White, R. S., Winder, T., gstsdttir, T., 2020. Seismicity of the askja and brarbunga volcanic systems of iceland, 20092015. Journal of Volcanology and Geothermal Research 391, 106432.

Guidoboni, E., Ciuccarelli, C., 2011. The campi flegrei caldera: historical revision and new data on seismic crises, bradyseisms, the monte nuovo eruption and ensuing earthquakes (twelfth century 1582 ad). Bulletin of volcanology 73 (6), 655–677.

Macedonio, G., Giudicepietro, F., D'auria, L., Martini, M., 2014. Sill in-

trusion as a source mechanism of unrest at volcanic calderas. Journal of Geophysical Research: Solid Earth 119 (5), 3986–4000.

Ogata, Y., Katsura, K., 1993. Analysis of temporal and spatial heterogeneity of magnitude frequency distribution inferred from earthquake catalogues. Geophysical Journal International 113 (3), 727–738.

Orazi, M., D?Auria, L., Tramelli, A., Buonocunto, C., Capello, M., Caputo, A., De Cesare, W., Giudicepietro, F., Martini, M., Peluso, R., et al., 2013. The seismic monitoring network of mt. vesuvius. Annals of Geophysics 56 (4), 0450.

Orsi, G., Civetta, L., Del Gaudio, C., de Vita, S., Di Vito, M., Isaia, R., Petrazzuoli, S., Ricciardi, G., Ricco, C., 2004. Short-term ground deformations and seismicity in the resurgent campi flegrei caldera (italy): an example of active block-resurgence in a densely populated area. J. Volcanol. Geoth. Res. 91, 415–451.

Petrosino, S., De Siena, L., Del Pezzo, E., 2008. Re-calibration of the magnitude scales at Campi Flegrei, Italy, on the basis of measured path and site and transfer functions. Bull. Seismol. Soc. Am. 98 (4), 1964–1974.

Shi, Y., Bolt, B. A., 1982. The standard error of the magnitude-frequency b value. Bulletin of the Seismological Society of America 72 (5), 1677–1687.

Siniscalchi, A., Tripaldi, S., Romano, G., Chiodini, G., Improta, L., Petrillo, Z., D'Auria, L., Caliro, S., Avino, R., 2019. Reservoir structure and hydraulic properties of the campi flegrei geothermal system inferred by au-

diomagnetotelluric, geochemical, and seismicity study. Journal of Geophysical Research: Solid Earth 124 (6), 5336–5356.

Tramelli, A., Troise, C., De Natale, G., Orazi, M., 2013. A new method for optimization and testing of microseismic networks: an application to Campi Flegrei (Southern Italy). Bull. Seismol. Soc. Am. (3).

Vitale, S., Isaia, R., Ciarcia, S., Giuseppe, M., Iannuzzi, E., Prinzi, E., Tramparulo, F., Troiano, A., 05 2019. Seismically induced soft-sediment deformation phenomena during the volcano-tectonic activity of campi flegrei caldera (southern italy) in the last 15 kyr. Tectonics.

Wiemer, S., Wyss, M., 2000. Minimum magnitude of complete reporting in earthquake catalogs: examples from Alaska, the Western United States and Japan. Bull. Seismol. Soc. Am. 90, 859869.

Woessner, J., Wiemer, S., 2005. Assessing the quality of earthquake catalogs: estimating the magnitude of completeness and its uncertainties. Bull. Seismol. Soc. Am. 95, 684–698.

Zaccarelli, L., Bianco, F., 2017. Noise-based seismic monitoring of the campi flegrei caldera. Geophysical Research Letters 44 (5), 2237–2244.

Zollo, A., Judenherc, S., Auger, E., D'Auria, L., Virieux, J., Capuano, P., Chiarabba, C., de Franco, R., Makris, J., Michelini, A., Musacchio, G., 2003. Evidence for the buried rim of Campi Flegrei caldera from 3-d active seismic imaging. Geophys. Res. Lett. 30 (19), doi:10.1029/2003GL018173.

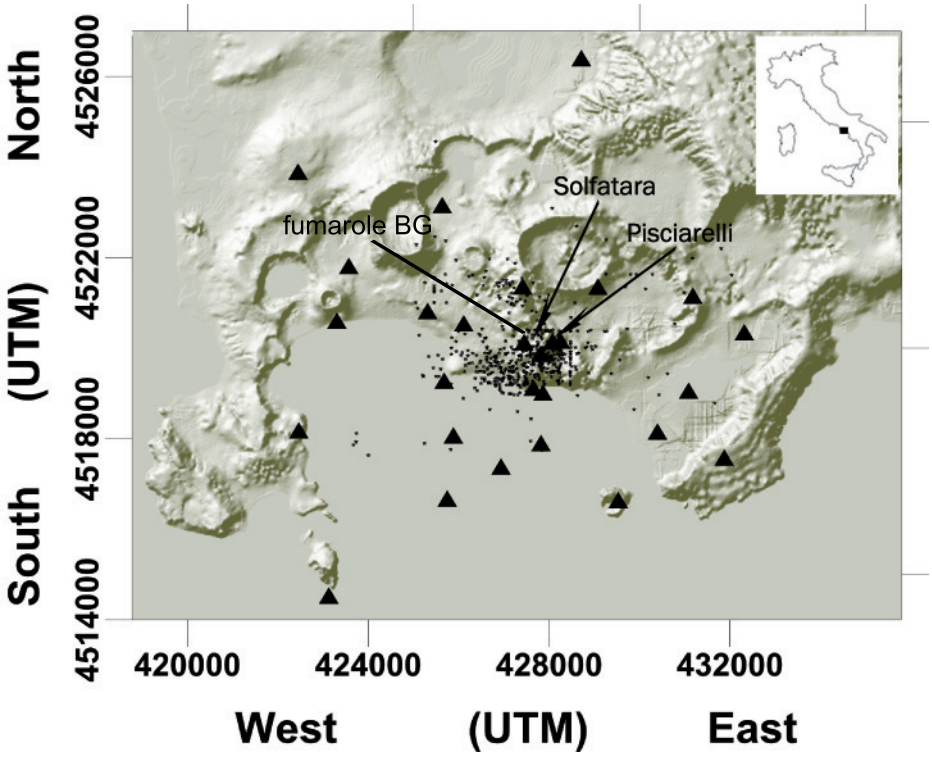

Figure 1: Map of the Campi Flegrei with seismic stations (triangles) and earthquakes (little stars) positions. Pisciarelli and Solfatara vents are indicated with arrows.

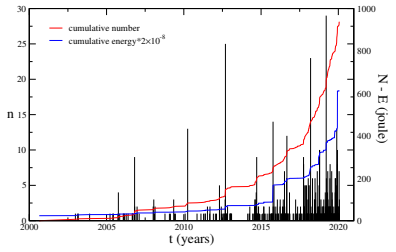

Figure 2: Histogram of the earthquakes per day (black), cumulative of the earthquakes number (red) and cumulative of the energy released (blue).

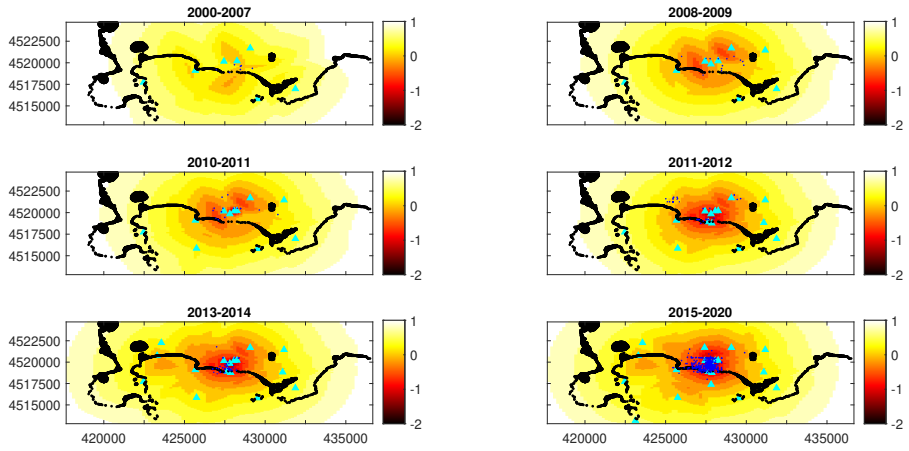

Figure 3: Temporal variations of the sensibility to location of the seismic network.

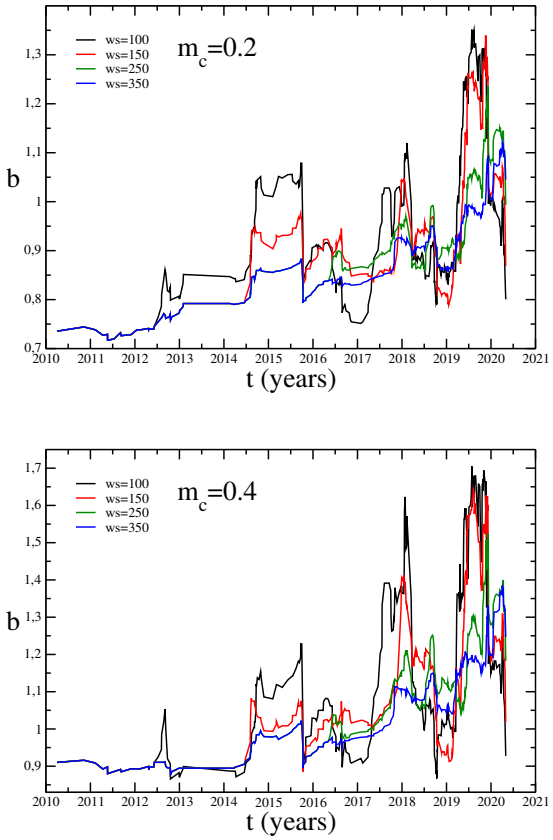

Figure 4: Temporal variations of the b value for different window size and M_c values.

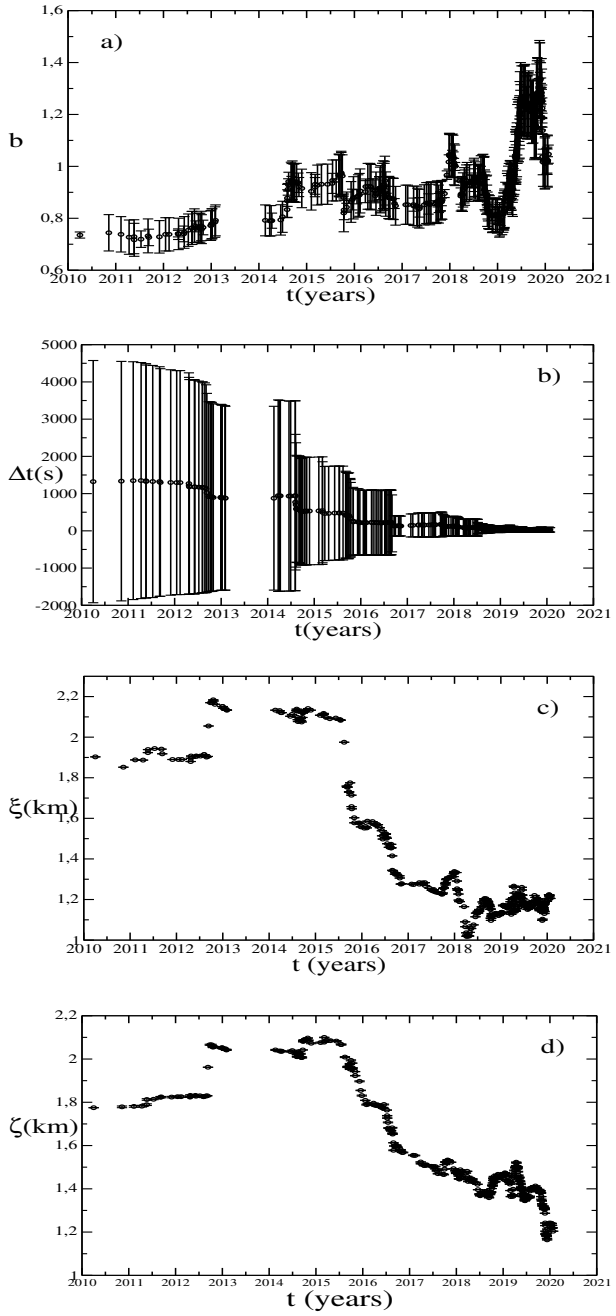

Figure 5: Temporal variation of (a) b-value with its standard deviation calculated following Shi and Bolt (1982); (b) inter-time; (c) and (d) epicentral inter-distance and average depth, respectively. Error bars represent the standard deviations.

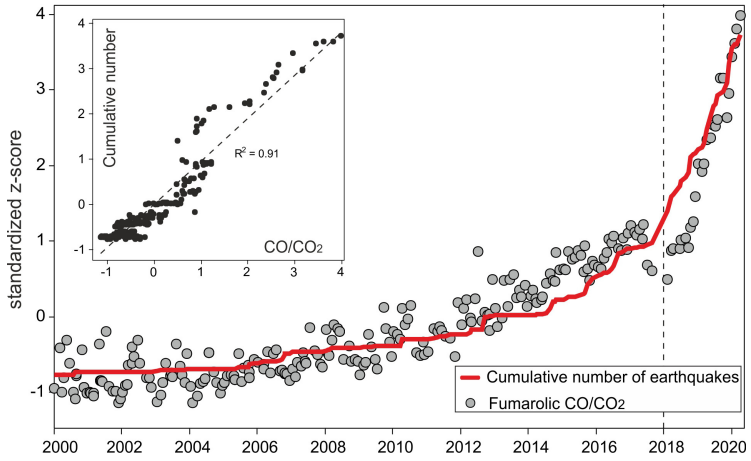

Figure 6: CO/CO_2 fumarolic ratio and cumulative number of earthquakes normalized with the z-score method. The inside panel shows the same variables one vs the other.

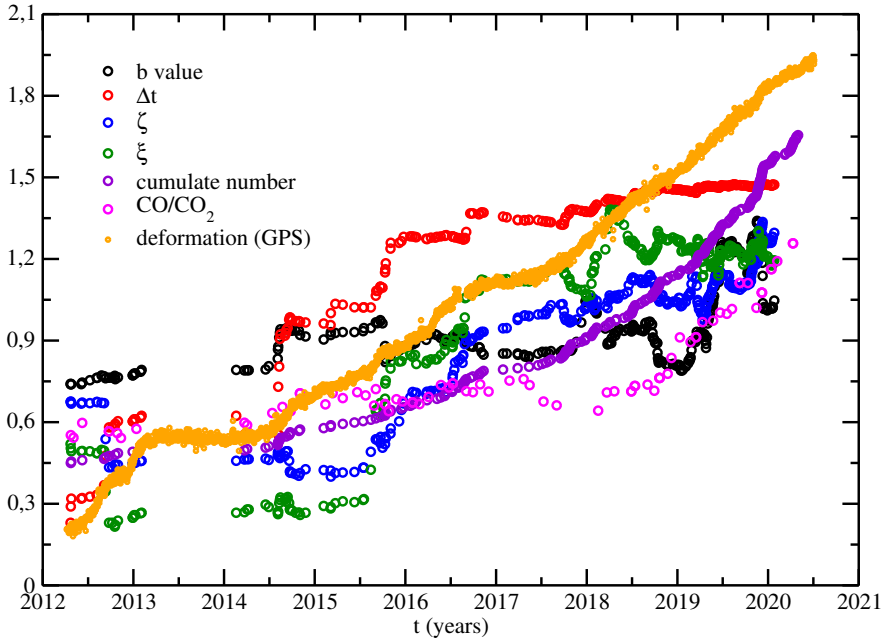

Figure 7: Temporal variations of all variables. Decreasing curves (see Fig.5) have been multiplied by -1. All curves have been shifted and/or rescaled in order to plot all the variables on the same scale.

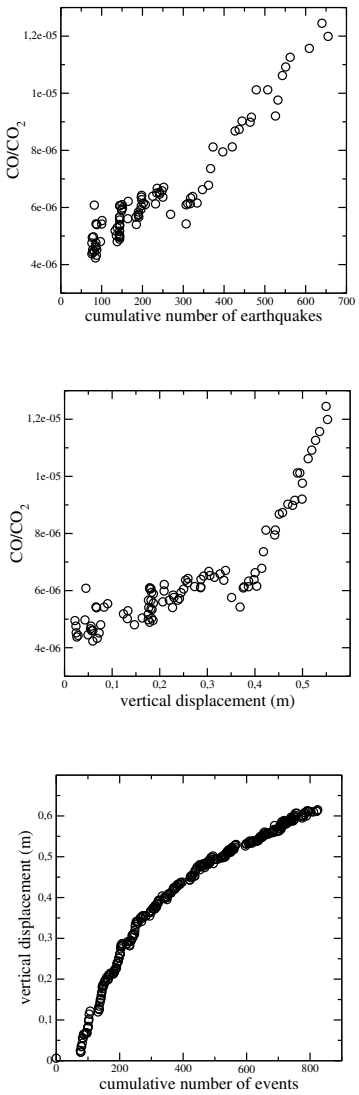

Figure 8: CO/CO_2 fumarolic ratio versus the cumulative number of earthquakes, CO/CO_2 fumarolic ratio versus the vertical displacement and the vertical displacement versus the cumulative number of earthquakes. In all cases the correlation between the variables appears to be very clear independently of the functional form of the dependence.

Figures

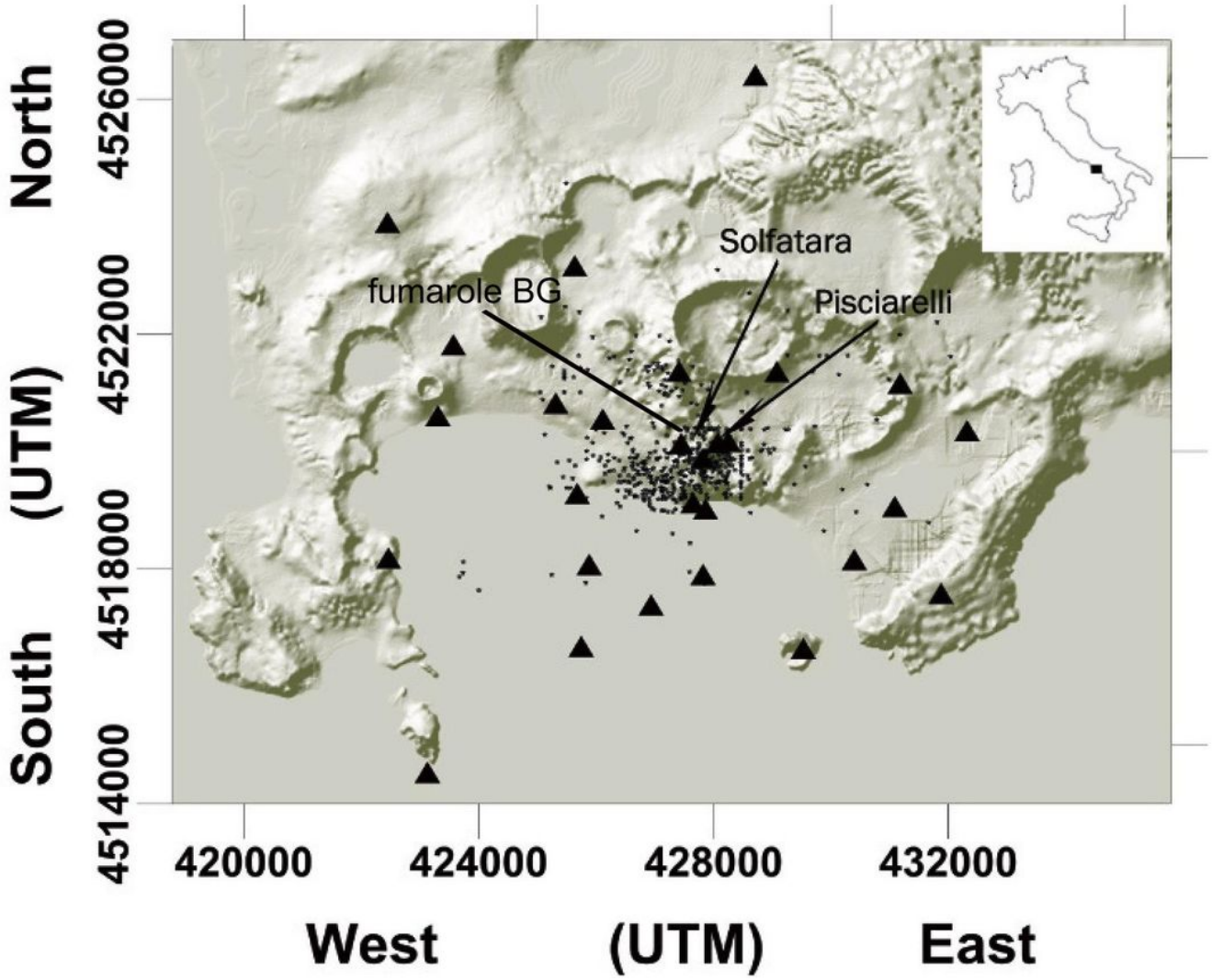

Figure 1

Map of the Campi Flegrei with seismic stations (triangles) and earthquakes (little stars) positions. Pisciarelli and Solfatara vents are indicated with arrows. Note: The designations employed and the presentation of the material on this map do not imply the expression of any opinion whatsoever on the part of Research Square concerning the legal status of any country, territory, city or area or of its authorities, or concerning the delimitation of its frontiers or boundaries. This map has been provided by the authors.

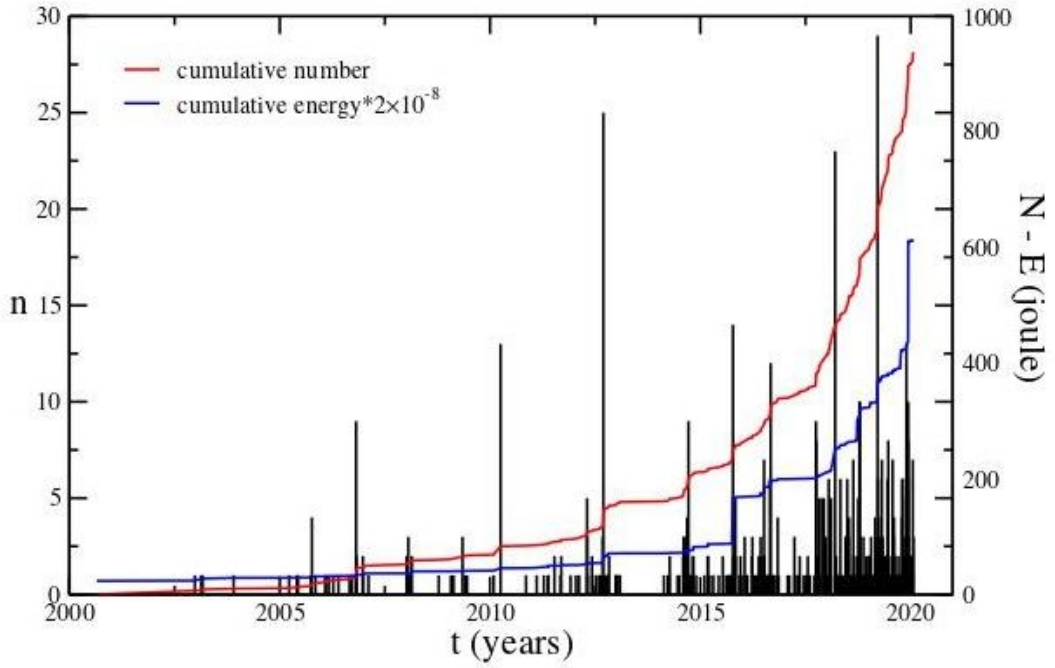

Figure 2

Histogram of the earthquakes per day (black), cumulative of the earthquakes number (red) and cumulative of the energy released (blue).

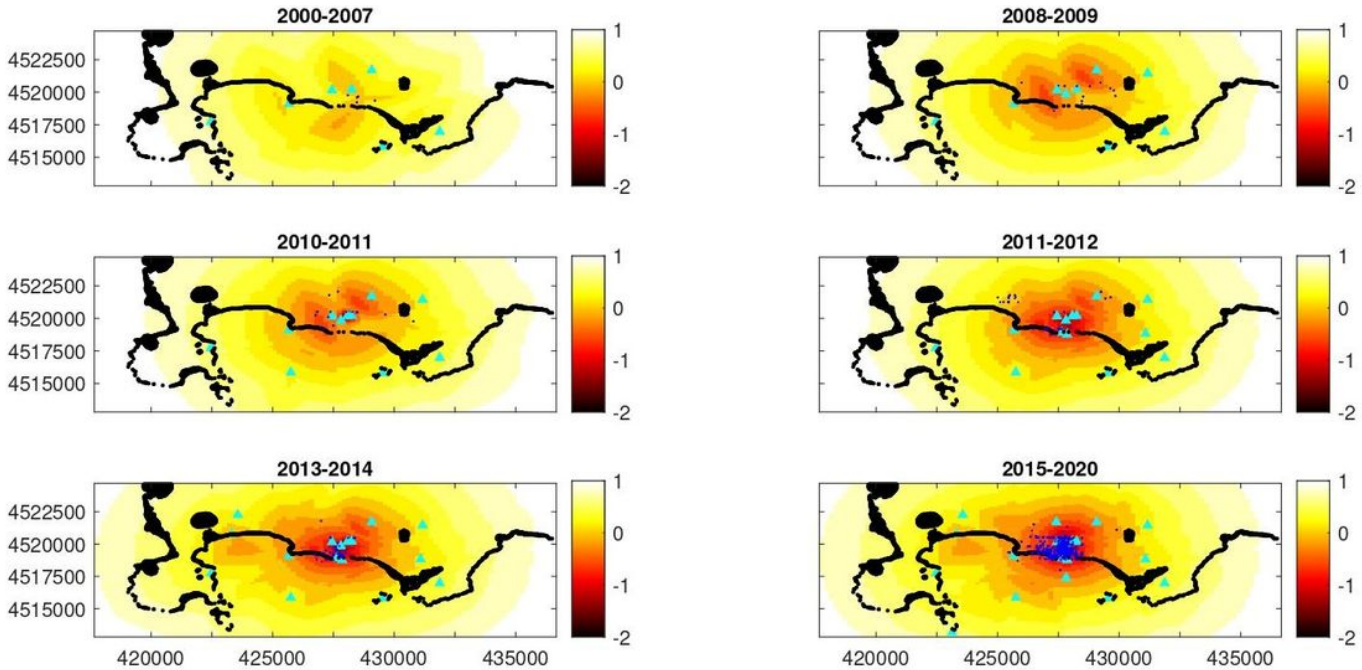

Figure 3

Temporal variations of the sensibility to location of the seismic network.

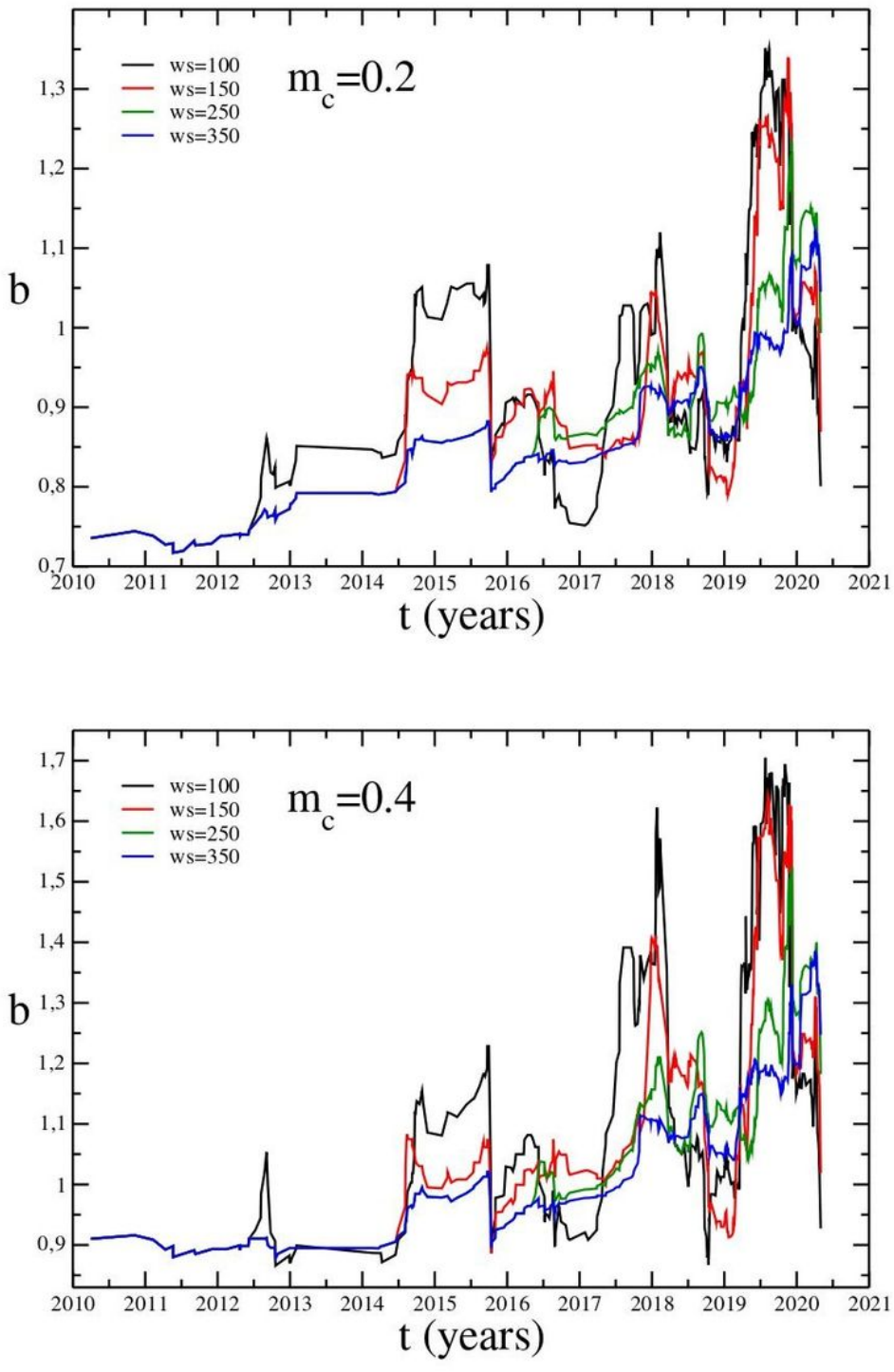

Figure 4

Temporal variations of the b value for different window size and Mc values.

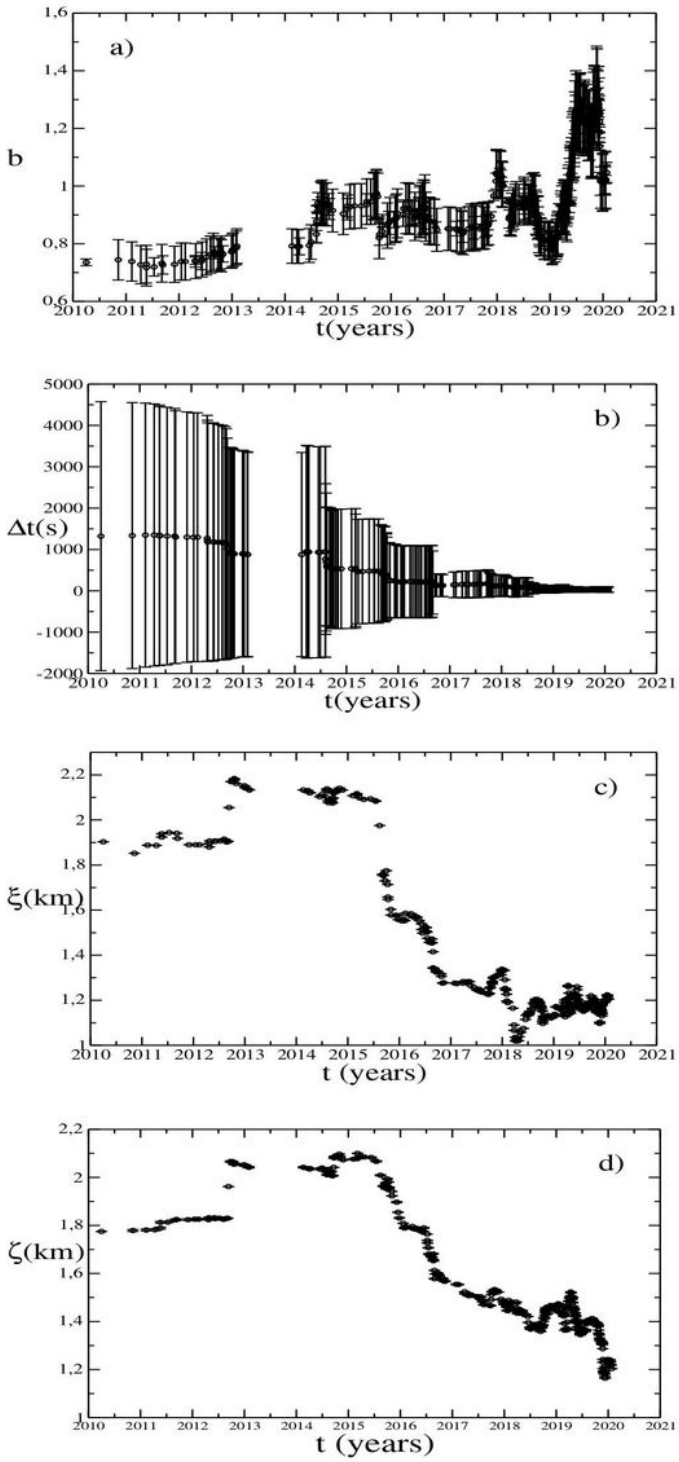

Figure 5

Temporal variation of (a) b-value with its standard deviation calculated following Shi and Bolt (1982); (b) inter-time; (c) and (d) epicentral inter-distance and average depth, respectively. Error bars represent the standard deviations.

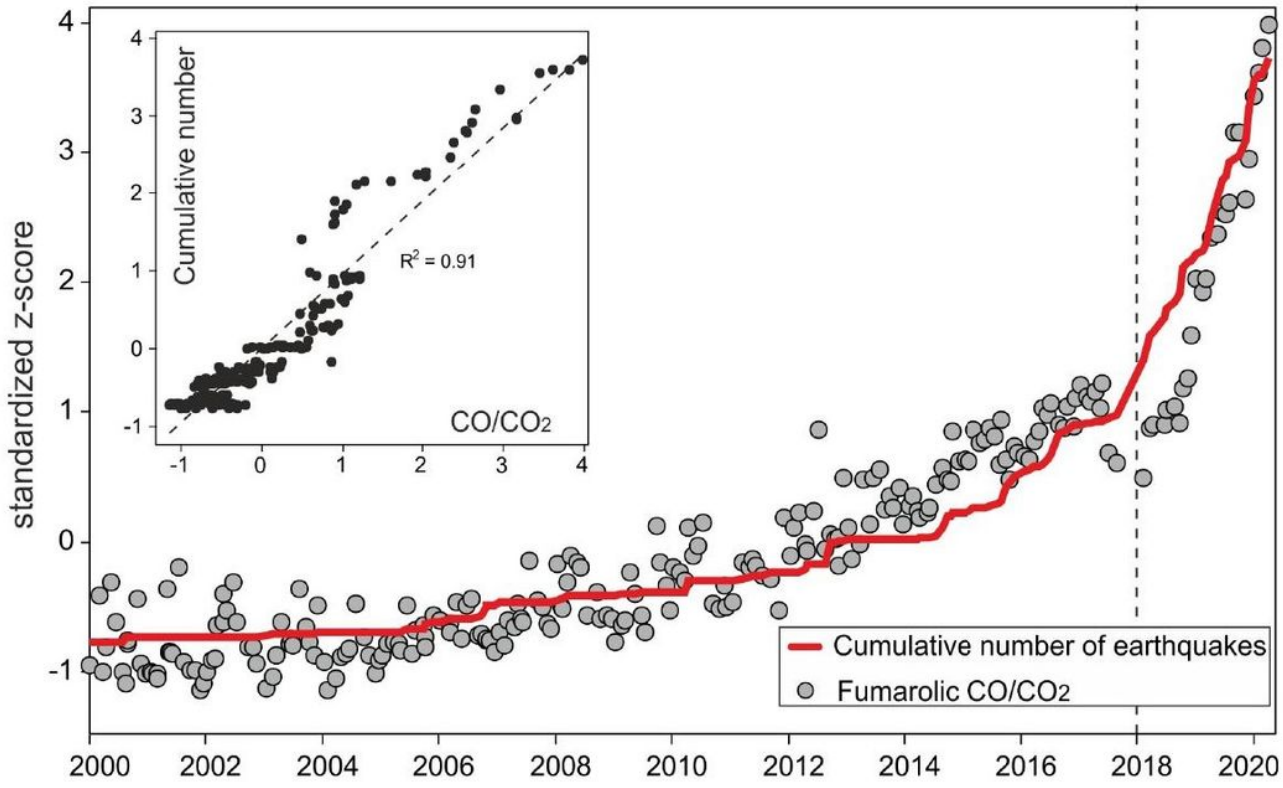

Figure 6

CO/CO2 fumarolic ratio and cumulative number of earthquakes normalized with the z-score method. The inside panel shows the same variables one vs the other.

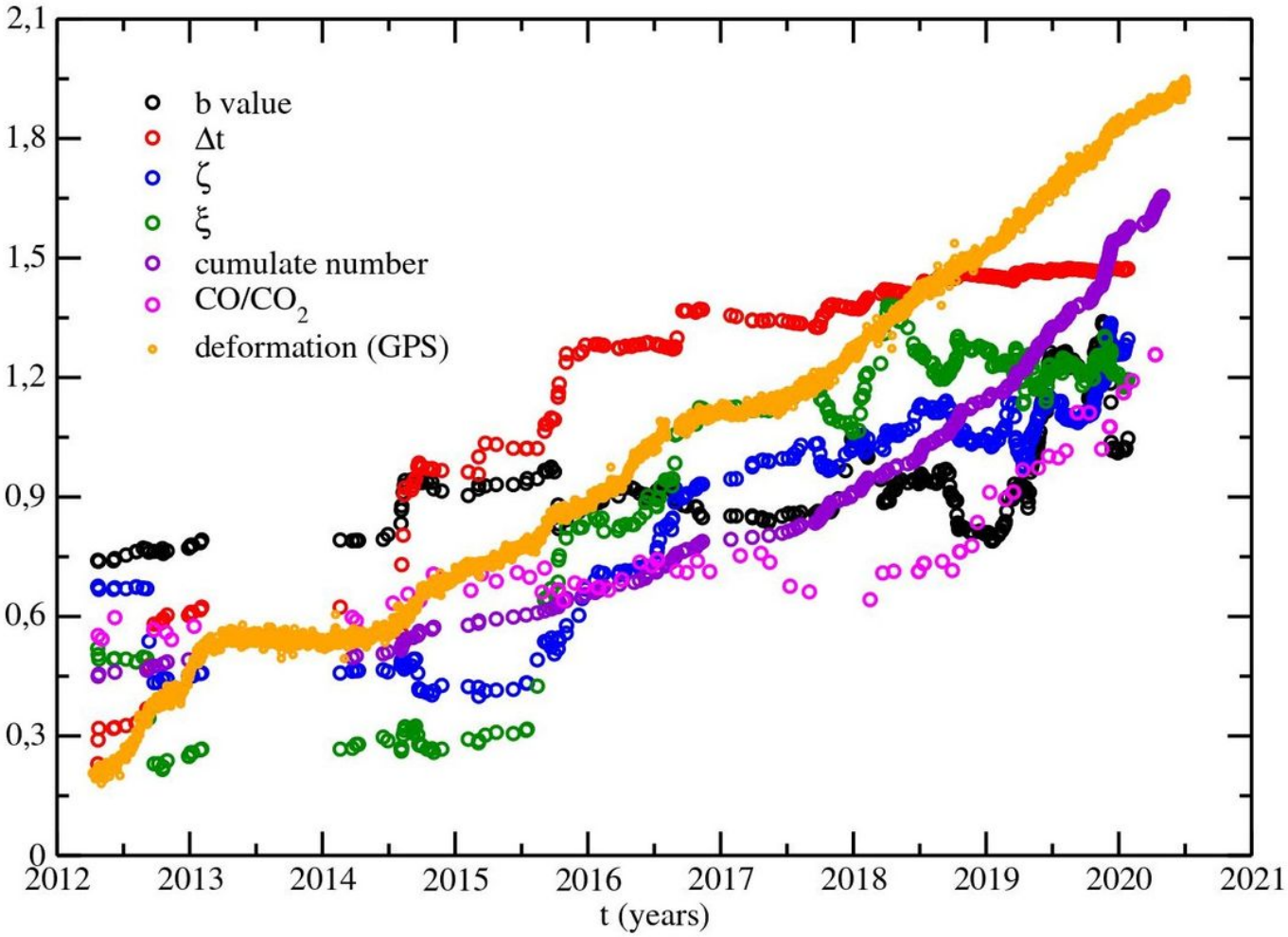

Figure 7

Temporal variations of all variables. Decreasing curves (see Fig.5) have been multiplied by -1. All curves have been shifted and/or rescaled in order to plot all the variables on the same scale.

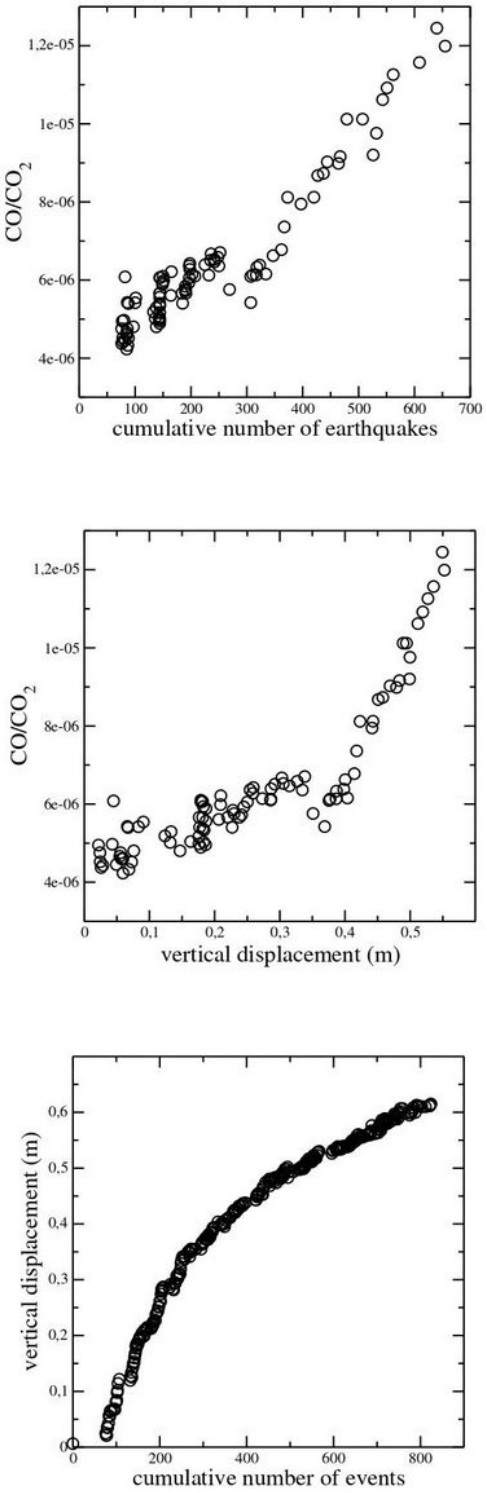

Figure 8

CO/CO2 fumarolic ratio versus the cumulative number of earthquakes, CO/CO2 fumarolic ratio versus the vertical displacement and the vertical displacement versus the cumulative number of earthquakes. In all cases the correlation between the variables appears to be very clear independently of the functional form of the dependence.

Supplementary Files

This is a list of supplementary files associated with this preprint. Click to download.

- suppmaterials2.pdf